Multi-cluster decays of heavy nuclei – studies in progress

D.V. Kamanin[*], Yu.V. Pyatkov[*,†], W. von Oertzen[**], A.A. Alexandrov[*], I.A. Alexandrova[*], O.V. Falomkina[*,‡], N. Jacobs[§], N.A. Kondratjev[*], Yu.N. Kopatch[*], E.A. Kuznetsova[*], Yu.E. Lavrova[†], V. Malaza[§], S. Mullins[¶], A.N. Tyukavkin[†], W. Trzaska[‖] and V.E. Zhuchko[*]

[*]*Joint Institute for Nuclear Research, 141980 Dubna, Moscow Region, Russia*
[†]*National Nuclear Research University MEPHI, 115409 Moscow, Russia*
[**]*Helmholtz-Zentrum Berlin, Glienickerstr. 100, 14109 Berlin, also Fachbereich Physik, Freie Universität*
[‡]*Lomonosov Moscow State University, Physics Faculty, Computer Methods in Physics Division, 119899, Russia*
[§]*Faculty of Military Science, Military Academy, Saldanha 7395, South Africa*
[¶]*iThemba Laboratory for Accelerator Based Sciences, Somerset West 7129, South Africa*
[‖]*Department of Physics of University of Jyväskylä, Finland*

Abstract. Experimental results in favour of the existence of a new type of cluster decay called "collinear cluster tri-partition", CCT, are presented. They are based on two different experiments with binary coincidences and measurements of the masses and energies of the two fragments, as well as using in one of the experiments observables sensitive to the nuclear charge of the fission fragments. A relatively high yield of the CCT-effect (more than 10^{-3} per binary fission) is likely due to the favourable Q-values (more positive than binary) and is expected due to a collective motion through very elongated (hyper-deformed) pre-scission shapes of the mother system. The process is considered to result from a sequential process, where a heavy cluster (lead as in the case of known cluster radioactivity) is replaced by pairs of two lighter clusters such as the magic isotopes of Sn/Ni or Sn/Ge.

Keywords: ternary fission, cluster decay
PACS: 23.70.+j; 25.85.Ca; 25.85.Ec

INTRODUCTION

Nuclear fission, a process where a heavy nucleus decays into two fragments of intermediate mass (e.g. Ba + Kr) has been identified by Hahn and Strassmann in 1938. It was discovered by chemical analysis while iradiating natural Uranium with thermal neutrons [1]. Shortly afterwards Petrzhak and Flerov [2] observed spontaneous fission of the ^{238}U isotope. The energy release in the fission process was immediately calculated by all leading physicists at that time to be very large, typically 200–205 MeV (e.g. Meitner and Frisch [3]). The large value is due to the larger binding energy per nucleon (E_B/N) in the mass range around mass $A = 54$ (iron, $E_B/N = 8.2$ MeV), as compared to the value at the end of the periodic table, $E_B/N = 7.2$ MeV. This fact could have been noticed four years before these discoveries, because of the existence of the liquid drop model and the nuclear mass formula of Bethe and Weizsäcker [4]. However, the large collective motion through a large deformation (today called super-deformation) was considered to

be unlikely.

Fission of heavy low-excited nuclei into three fragments of comparable masses, so called "true ternary fission", has been intensively investigated soon after the discovery of fission. Swiatecki [5] has shown within the framework of the liquid drop model that fission into three heavy fragments is energetically more favourable than binary fission for all nuclei with fission parameters $30.5 < Z^2 / A < 43.3$. In 1963 Strutinsky [6] has calculated the equilibrium shapes of the fissioning nucleus and has shown, that along with the ordinary configuration with one neck, there is the possibility of more complicated elongated configurations with two and even three necks, at the same time it was stressed, that such configurations are much less probable. Later Diehl and Greiner [7, 8] have shown a preference for prolate over oblate saddle-point shapes for the fission of a nucleus into three fragments of similar size. Such pre-scission configurations could lead to almost collinear separation of the decay partners, at least in a sequential fission process. Actually the Coulomb interaction in the total potential energy is the smallest for linear arrangements of the three fragments. Furthermore results demonstrating a decisive role of shell effects in the formation of the multi-body chain-like nuclear molecules were obtained also by Poenaru et al. [9].

On the experimental side there have been multiple attempts to find the true ternary fission in low energy fission by means of counting techniques and in radiochemical studies. The schemes of the spectrometric experiments were based on the assumption of comparable angles between all three fragments emitted [10, 11]. Masses of the fragments were calculated in this case based on experimental values of the energies and angles. Contradictory results have been obtained; these were treated as showing the absence of fission fragments in the vicinity of mass fifty both in binary and ternary fission [12]. At the same time almost collinear ternary decays of excited heavy nuclear systems were known from the experiments in Ref. [13, 14] at the early stage of our work.

Bearing in mind the results mentioned above, we came to the conclusion, that collinear tri-partition of low-excited heavy nuclear systems would be a promising field of research. In our first experiments dedicated to this problem [15, 16] some indications of such processes were already observed. At least one of the decay products detected was a magic nucleus. By analogy with known cluster decay (or lead radioactivity), the process has been called "collinear cluster tri-partition" (CCT).

EXPERIMENTS

In the present work we describe the results of two different experiments devoted to the search for collinear tri-partition of heavy nuclei. In these experiments binary coincidences with two detector systems placed at relative angles of 180^0 are measured, see Figs. 1 and 2. Among all known detection methods to measure the masses of nuclear reaction products, the TOF-E (time-of-flight *vs* energy) method is the only one which uniquely allows the study of multi-body decays. In this method both, the fragment velocities V, obtained by means of TOF and the energy E, are measured for each detected fragment individually. The fragment mass M_{TE} is calculated simply using the equation $M_{TE} = 2E/V^2$. For a three-body decay six variables determine the kinematics (e.g. 3 masses and 3 velocities). Adding momentum and energy conservation reduces the num-

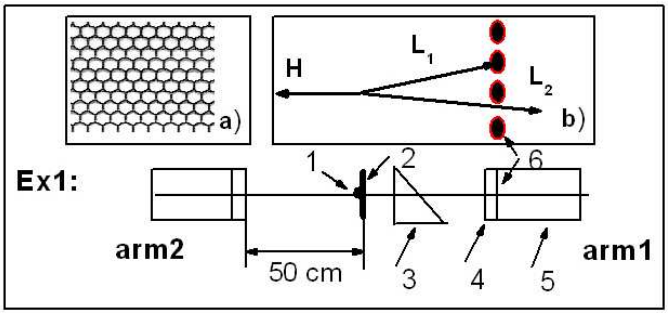

FIGURE 1. Scheme of (Ex1) for coincidence measurements of two fragments of the fission decay of ^{252}Cf. This experiment has been performed at the FOBOS setup [17]. Here: 1 – Cf source, 2 – source backing, 3 – micro-channel plate (MCP) based timing "start" detector, 4 – position sensitive avalanche counter (PSAC) as "stop" detector, 5 – ionization chamber (BIC) with the supporting mesh, 6 – the mesh of the entrance window. The front view of the mesh is shown in the insert a), an enlarged mesh section is presented in the insert b). After passage of the two fragments through the source backing, two light fragments L_1 and L_2, are obtained with a small angle divergence due to multiple scattering. In (b) we show that one of the fragments (L_1) can be lost hitting the metal structure of the mesh, while the fragment L_2 reaches the detectors of the arm 1. The source backing (2) exists only on one side and causes the mentioned angular dispersion in the direction towards the right arm1.

ber of independent variables to four. In our experiments two masses and two velocities are determined for two fragments observed at a relative angle of 180^0. All the results presented below are obtained within the framework of the "missing–mass" approach. With the two-arm spectrometers binary coincidences have been measured, with a special mechanism, which blocks the registration of a third fragment, as explained below and in Fig.1. This means that only two fragments were actually detected in each fission event and their total mass, the sum M_s will serve as a sign of a multi-body decay if it is significantly smaller than the mass of the initial system.

Experiment Ex1

In the first experiment (Ex1, Fig. 1), performed at the FOBOS [17] setup in the Flerov Laboratory of Nuclear Reactions (FLNR) of the Joint Institute for Nuclear Research (JINR) in Dubna [17], about 13×10^6 coincident binary fission events of ^{252}Cf were collected. The TOF of the fragment was measured over a flight path of 50 cm between the "start" detector, label (3) in Fig. 1, which is based on micro-channel plates (MCP) placed next to the ^{252}Cf-source and "stop" obtained by position sensitive avalanche counters (PSAC, 4). The source activity was 370 fissions/sec, it was deposited on a Al_2O_3 backing of 50 $\mu g/cm^2$ thickness and 18 mm in diameter – (1). Through the measurements of the position of the fragments in the PSAC's, this information provided also the fragment's emission angle with a prescission of 1^0. The energies of those coincident fragments which passed through the PSACs were measured in the Bragg ionization chambers (BIC, label 5 in Fig. 1). The entrance windows of the large BIC are made of 1 μm thick aluminized Mylar, with a diameter of 385 mm. To withstand the pressure of the counting gas, the delicate window foil has to be supported by a two-

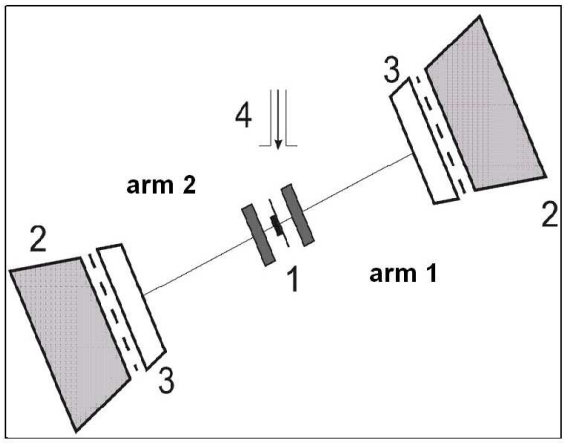

FIGURE 2. The scheme (Ex2) of the mini-FOBOS spectrometer which includes a "start" avalanche counter with an internal target (1), Bragg ionization chambers (BIC) (2) and "stop" position-sensitive avalanche counters (PSAC) (3). The target is irradiated by a collimated beam of thermal neutrons (4).

fold structure – a concentric heavy carrier of a transparency of 94% and an adjacent etched Ni-mesh having a cell dimension of 2.7 mm in diameter and 0.9 mm bulkhead in between the open pores. The thickness of the mesh is about 1 mm. The geometrical structure of the mesh is hexagonal, its front view is shown in the insert, a), of Fig. 1, a mesh section is presented in the insert b). The mesh reduces the total transparency to 75%. This mesh is a very important peculiarity of the present experiments as explained below (see Fig. 1).

Experiment Ex2

For a better understanding of the unusual decay channel in ^{252}Cf (sf) we planned to investigate different fissile systems at different excitation energies up to the threshold of the survival of nuclear shells. One of the reactions we had chosen in an additional experiment was fission induced by thermal neutrons in ^{235}U(n_{th}, f).

The experiment (Ex2) was performed with a beam of thermal neutrons of the IBR-2 reactor in the Frank Laboratory of Neutron Physics of the JINR with the help of the double-armed TOF-*E setup* in the mini-FOBOS [18] spectrometer. The overall statistics processed in this experiment *was* about 2×10^6 fission events. The scheme of the setup is shown in Fig. 2. The spectrometer is also based on FOBOS detector modules. The start detector is a symmetrical avalanche counter with an internal target. An active layer of the target material was prepared by evaporation of 100 μg/cm^2 of ^{235}U on an Al_2O_3 backing of 50 μg/cm^2 thickness. In this case along with measuring the fission fragment (FF) time-of-flight (TOF) and their energies (E), two more parameters being sensitive to the nuclear charge are added. The drift time of a track formed after stopping of a fragment in the gas volume of the BIC is known to be linked with the fragment nuclear charge [19]. The corresponding parameter was measured as the time difference between the PSAC signal and the signal from the Frisch grid of the BIC. Special calibration procedures

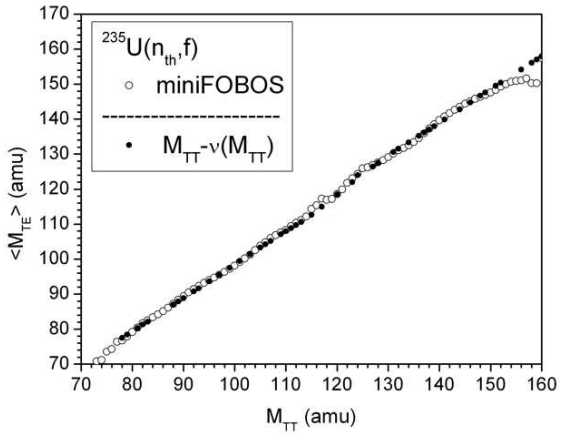

FIGURE 3. Correlation of the mean values of the experimental mass $<M_{TE}>$ (post-neutron emission) *vs* mass ,M_{TT}, obtained in the present TOF-TOF analysis. The shift due to neutron emission $\nu(M_{TT})$ [22] has been taken into account.

have been worked out for the FF nuclear charge determination [20]. According to the tests carried out before, the charge resolution does not exceed 3.8 units (FWHM) for the FF from the light mass peak, while the mean values for each fixed charge are correctly determined.

The second independent variable, which is also sensitive to the nuclear charge, is the specific energy loss of the FF in the gas volume of the PSAC [17]. This parameter proved to be very useful also for the selection of the CCT events.

In both experiments similar procedures for the TOF-E calibration and the calculation of the M_{TE} masses were used. In brief, the mass spectrum of binary decays, which depends on the measured variables and parameters to be determined, was forced to fit the known mass spectrum of ^{252}Cf fission [21]. The data presented in Fig. 3 were obtained in the following way. For each fixed experimental M_{TT}(TOF, TOF) mass a corresponding mean value of M_{TE} was obtained. $M_{TT}{}^{(1)}$ (primary i.e. before neutron emission fragment mass) was calculated as $M^{(1)}{}_{TT} = M_c/\,(1 + V_1/V_2)$, where M_c – the mass of the fissioning system, $V_{1,2}$ – velocities of the coincident fragments (indexes correspond to the numbers of the spectrometer arms). The values $<M_{TE}>$ are compared with the value expected for i.e. M_{TT} - $\nu(M_{TT})$, where $\nu(M_{TT})$ – mean number of neutrons emitted from the fragment with mass M_{TT}, taken from Ref. [22]. Thus, Fig. 3 demonstrates an absence of shifts (essential nonlinearity) in the calibration of the M_{TE} masses. This point is very important for the correct treatment of the data, especially for the mass characteristics and the peculiarities discussed below such as peaks and ridges in the spectra and distributions, respectively.

RESULTS AND ANALYSIS

The analysis is based on the presentation and discussion of two-dimensional diagrams of the registered masses (M_1 and M_2), in which the sum M_s of the two masses can be discussed. The events with total masses $M_s = M_1 + M_2$ will appear as diagonal lines in

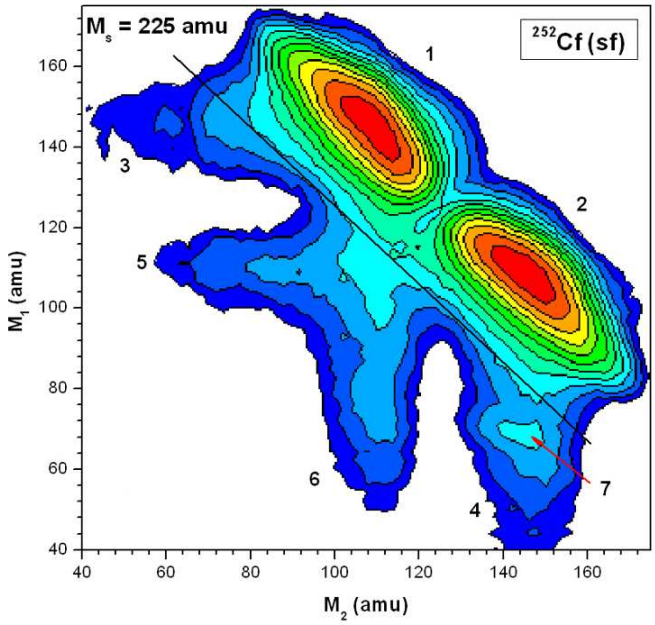

FIGURE 4. (Color online) Contour maps (in logarithmic scale, the steps between colors are approximately a factor 2.5) of the mass-mass distribution of the collinear fragments, detected in coincidence in the two opposite arms of the FOBOS spectrometer in (Ex1). The additional bump (7) in arm1 is inducated by an arrow. See text for more details.

the mass correlation plot. From these two-dimensional presentations further projections onto the individual axes M_1 or M_2 are made.

Results of experiment Ex1, ^{252}Cf (sf)

Fig. 4 shows in a logarithmic scale the two-dimensional distribution ($M_2 - M_1$) of the two registered masses of the coincident fragments in the experiment (Ex1). In this FOBOS setup M_1 is defined as the fragment mass derived from the arm pointing to wards the detector arm with the additional dispersive (scattering) materials. Only collinear fission events with a relative angle of 180 ± 2^0 were selected, which corresponds to the typical angular spread for conventional binary fission fragments.

The "tails" in the mass distributions marked 3–6 in Fig. 4 extending from the regions (1) and (2) which are used to mark the conventional binary fission, are mainly due to the scattering of fragments on both the foils and on the grid edges of the "stop" avalanche counters and the ionization chambers. Once again we emphasize the small but important asymmetry in the experimental arrangement for the two arms, which consists in the thin source backing (50 μg/cm^2 of Al_2O_3) for the "rear side" of the target and the "start" detector foil located only in arm 1 (Fig. 4). An astonishing difference in the counting rate and in the shapes of the "tails" (3) and (4) attracts attention. In the case shown in Fig. 4 there is a distinct bump, marked (7), on top of the latter "tails" (4). The bump is located in a region corresponding to a large "missing" mass. In Fig. 4 the line for the measured

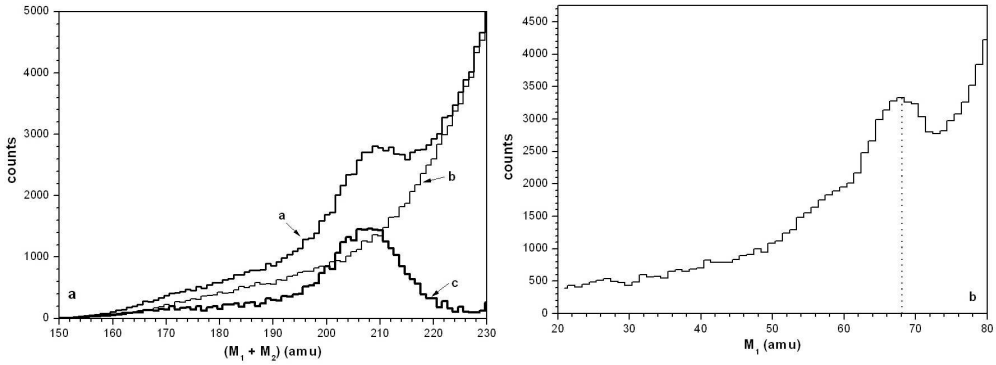

FIGURE 5. The bump "7" from (Ex1) in Fig. 4 is analyzed. In Fig. 5a) the spectra of the summed masses M_s for the "tails" (4 and 3) shown as spectrum *a* and *b*, respectively, are compared. The result of the subtraction of spectrum, b, from spectrum, a, (difference spectrum) is marked as c. On the rigth side, part b), the projection of the bump onto the M_1 axis is shown.

total mass $M_s = M_1 + M_2 = 225$ amu is shown as a border line separating these interesting events from normal binary fission. The statistical significance of the events in the structure (7) can be deduced from Fig. 5, where the spectra of total (summed) masses M_s for the "tails" (4) and (3) are compared. The yield of the events in the difference spectrum *c*, is $(4.7\pm0.2)\times10^{-3}$ relative to the total number of events in the distribution shown in Fig. 4. It is only a lower limit of the yield due to the reasons discussed below. In order to explain the differences in the "tails" (4) and (3) mentioned above (see also Fig. 7), the following scenario is proposed, the corresponding geometry has been shown in Fig. 1 (insert b). We assume that in ternary fission the three fragments are emitted collinearly due to two sequential binary decays. Two of the fragments are emitted in one direction but become separated in their velocity vectors with a small angle difference of $\sim1^0$ after passing the scattering media, due to multiple scattering [23]. These media are the backing of the source and the foil of the start detector both located only on the side of tail (4). For instance, for a ^{70}Ni fragment with the energy 70 MeV the mean angle of multiple scattering in the backing is equal to 0.64^0 while the tail of the angular distribution extends up to 2^0. As a result two fragments continue to fly in the same direction with a small angle divergence. It should be stressed that the influence of the backing onto the yield of ternary events was mentioned already in Ref. [11].

Thus, if both fragments pass on and enter into the (BIC), we register a signal corresponding to the sum of the energies of the two fragments. In this case the event will be treated as binary fission with the usual parameters. In the other cases only the proper energy (mass) of one of the light fragments is measured, because the second one is stopped (lost) in the supporting grid of the ionization chamber. Just the absence of a similar grid is likely the reason why the authors of the work in Ref. [24] have failed to observe collinear ternary decays of ^{252}Cf (sf) using the time-of-flight method.

For a more detailed analysis of the bump we have constructed the contour map of the two-dimensional mass-mass distribution obtained by subtraction of the "tail" (3) from the "tail" (4) (Fig. 6a). No additional normalization was used.

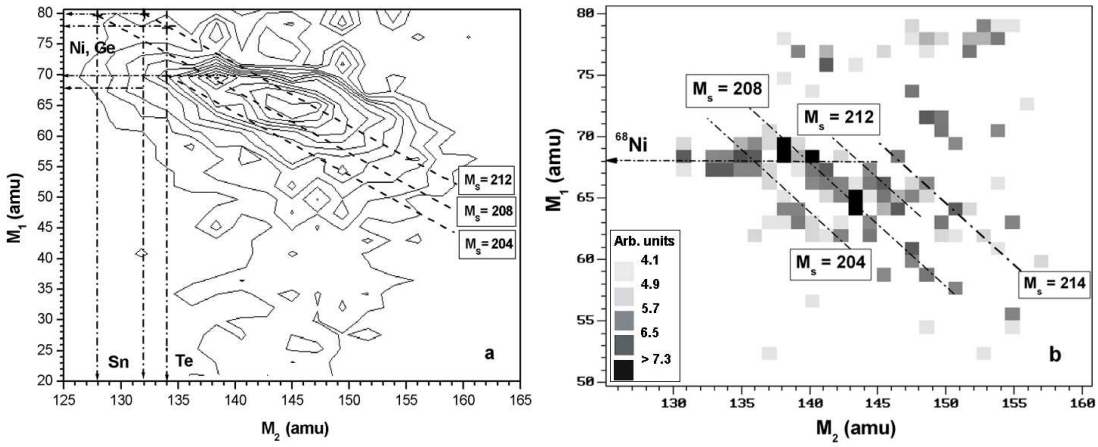

FIGURE 6. Left side, a).: The figure depicts as a $2D$-contour map (M_1 *vs* M_2) the difference between the "tails" (4) and (3), for the events measured in Ex1, with the system shown in Fig. 1; note the expanded scale for the lighter mass fragments (M_1). Dashed lines tilted by 45^0 with respect to the M_2 axis correspond to a fixed total mass of the two detected fragments $M_s = M_1 + M_2 =$ const. Part b): the same as in a), however, passed through a second derivative filter which emphasizes local peaks in each section of M_s = const. The ridges correspond to different values of M_s (204, 208, 212 and possibly 214 amu). The arrows in the figures mark positions of magic isotopes on the mass axis. Their role in the CCT process is discussed in the text.

This distribution is almost free from experimental background originating from scattered fragments of normal binary fission. Some features of this $2D$ plot can be further emphasized by a process, where a second derivative filter is applied (Fig. 6b), a method which is typically used in the search for peaks in gamma spectra and which is explained in more detail in Refs. [25, 26]. The vertical scale for the squares is defined in the insert to this figure. The maxima of the peaks extend over certain linear regions of M_2 = const, which are found predominantly as discrete diagonal lines, marked in Fig. 6b). Note that they correspond to the total masses $M_s =$ const with values of 204, 208, 212 and perhaps 214 amu, respectively. To show the positions of the tilted ridges on the map of the bump they are marked by the dashed lines in Fig. 6a). As can be deduced from the figure, the ridges go through crossing points corresponding to different combinations of two fragments with magic nucleon numbers (marked by the dot-dashed arrows). These marked points could be related to mass values with magic subsystems, well-known from binary fission [27, 28] as follows (corresponding Q values for ternary decays expressed in rounded numbers are marked in braces): $204 \rightarrow {}^{70}$Ni ($Z = 28$) + ^{134}Te {241 MeV} or ^{72}Ni + ^{132}Sn ($Z = 50$) {251 MeV}, $208 \rightarrow {}^{80}$Ge + ^{128}Sn {261 MeV} and for $212 \rightarrow {}^{80}$Ge + ^{132}Sn {257 MeV}, ^{78}Ni + ^{134}Te {228 MeV} or ^{68}Ni + ^{144}Ba {217 MeV} and for $M_s = 214 \rightarrow {}^{82}$Ge + ^{132}Sn {226 MeV}. It should be reminded that the Q value that corresponds to the most probable binary partition of ^{252}Cf is about 216 MeV.

Of course, at the moment this interpretation of the tilted ridges is only a hypothesis to be confirmed by other results shown below.

The ridges discussed are crossed as well by the horizontal ridge (seen via a bunching of contour lines in Fig. 6a). The projection of the bump onto the M_1 axis (Fig. 5b) confirms this conclusion. The effect can be linked with the isotopes of ^{68,70}Ni, which

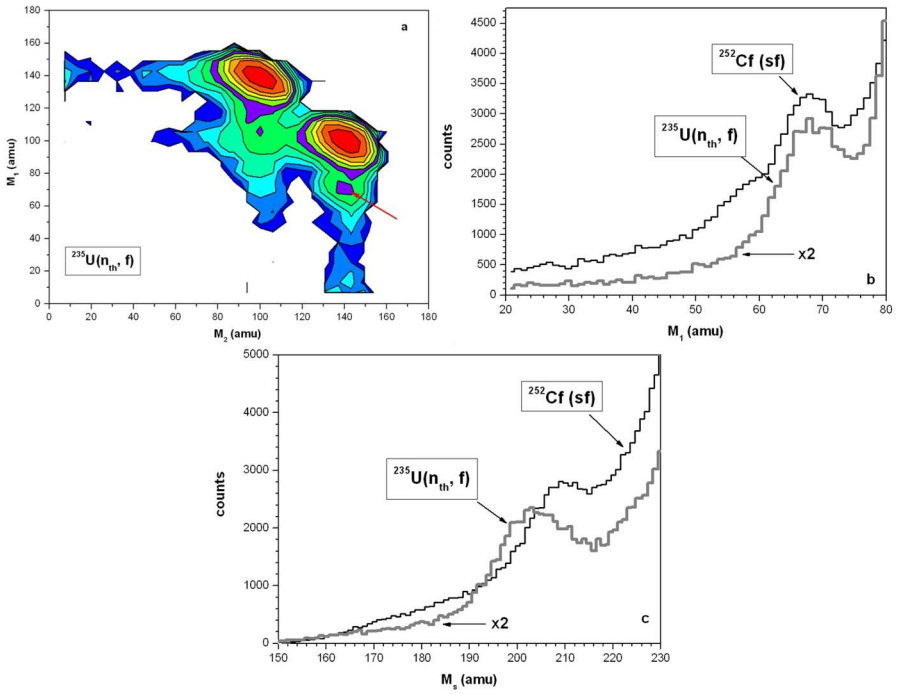

FIGURE 7. (Color online)a) The FF mass-mass distribution (logarithmic scale) obtained for the ^{235}U(n_{th},f) reaction. b) Projections of the bump onto the M_1 axis for comparison of the reactions discussed here. c) Projections of the bump onto the direction $M_s = M_2 + M_1 = \text{const}$.

are also magic [28].

Results of experiment Ex2, ^{235}U(n_{th},f)

The mere fact of the existence of the bump in the total mass on one side as discussed above, as well as the presence of its internal structure was confirmed in an experiment (Ex2) devoted to the ^{235}U(n_{th}, f) [29], in which nuclear charges were measured in addition.

A bump similar to that marked by an arrow in Fig. 4 is again well pronounced as shown in Fig. 7a). The yield of the events in the bump is $(5.1\pm0.4)\times10^{-3}$ relative to the total number of fission events detected. As in the previous case the bump is observed only in one spectrometer arm (marked by number 1) facing to the target backing. The projections of the bump onto the M_1 axis for both reactions are compared in Fig. 7b). The pronounced peaks in both cases are centered at the masses (68 ÷ 70) amu, associated with the magic isotopes of Ni. Projections onto the M_s = const direction are shown in Fig. 7c). Although the total masses of the corresponding two fissioning systems differ by 16 amu the projections of the bump onto this direction are shifted no greater than 6 amu. Such shift of the top yield in the frame of the wide peak could be assigned to the different population of the fission modes based on magic pairs of Sn/Ge or Sn/Ni isotopes in Cf and U* nuclei.

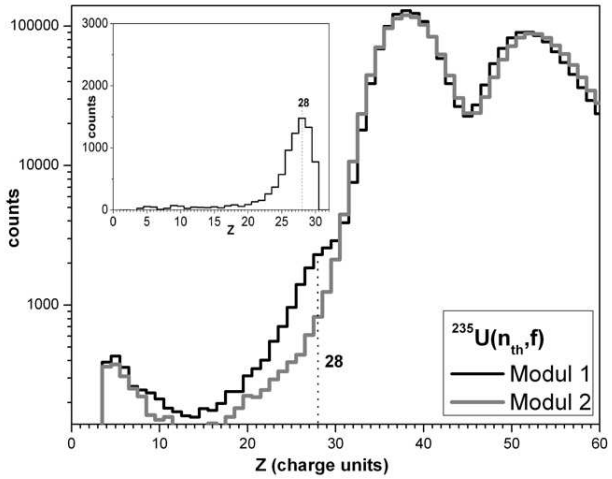

FIGURE 8. Nuclear charge spectra from the FF from the reaction ^{235}U(n_{th}, f), the FF are detected in the two opposite spectrometer arms. A difference in the yields (bump) presented in the upper panel in a linear scale is visible for the charges around Z = 28 (isotopes of Ni).

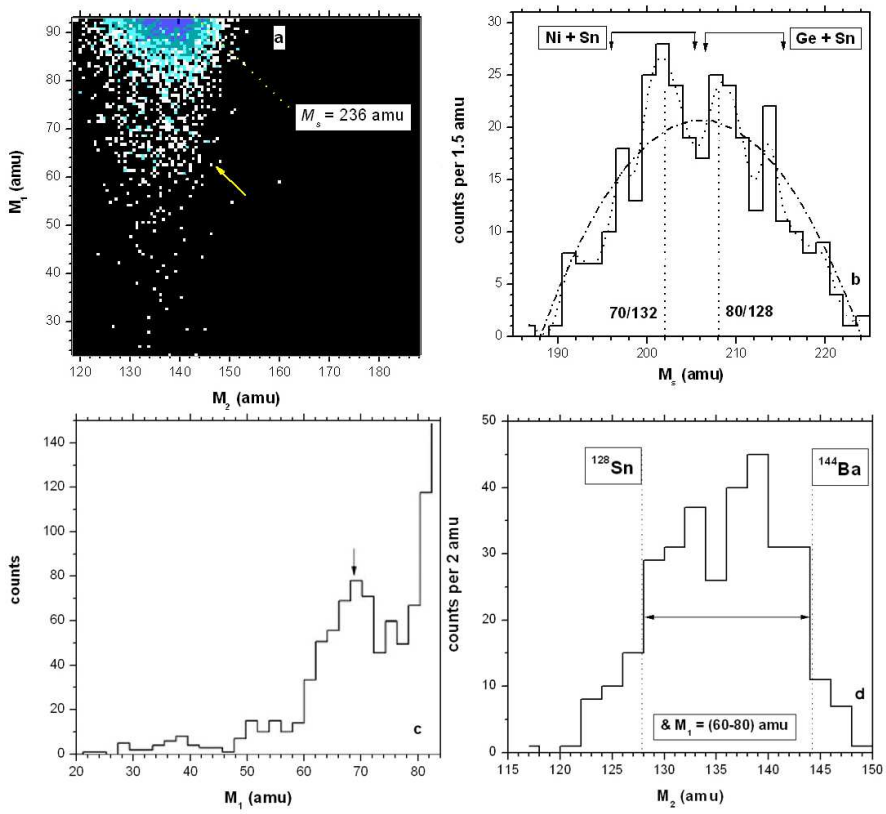

FIGURE 9. Upper row, a), mass-mass distribution of the fission events from the reaction ^{235}U(n_{th}, f) selected by the additional gate on the velocity-energy-loss, the V–dE matrix; b) Projection onto $M_1 + M_2$ = const direction. Parabolic and spline least squares fits are shown by dash-dot and dot lines respectively. c), Projection of the distribution onto M_1 axis; and d) Projection onto the M_2 axis for the events from the range M_1 = (60÷80) amu . See text for details.

We show the comparison of the spectra of nuclear charges of the measured FF in the two opposite spectrometer arms in Fig. 8. The result for the measured charges confirms the previous finding with the mass distributions, namely the existence of an additional bump in the arm with the scattering media. It confirms the hypothesis that the upper boundary of the additional bump (Fig. 7a), and b) is actually connected with Ni isotopes.

As was mentioned above, the presence of the tilted ridges M_s = const for the ^{252}Cf nucleus was revealed using a special mathematical process for the FF mass-mass distribution. This fact has been confirmed independently for the ^{236}U* system by using a selection with an additional parameter, the specific energy losses *dE* of the FF in the "stop" avalanche counter.

In Fig. 9 we show the mass-mass distribution of those FF, selected by the additional parameter of an increased energy loss in comparison to FF from the light mass peak of normal binary fission. In this way we can select the events when a "fork" of two fragments of a ternary decay fly into the same first spectrometer arm namely where the bump is observed. Total energy losses of these two fragments in the same counter have values, which are higher compared with the *dE* values for ordinary light fragments. It should be stressed that in this case the experimental variables used for gating (specific energy losses *vs* velocity) are not distorted due to scattering on the entrance grid of the BIC, being the main source of the background events.

In the bump region a tilted valley structure with reduced event density is clearly seen indicating the presence of ridges with specific total masses, M_s = const (Fig. 9a). It is marked by the tilted arrow. A projection of the bump onto this direction is shown in Fig. 9b), the left bracket in the spectrum shows the mass region of potential location of pairs of magic isotopes ^{128,132}Sn / ^{68,70,72}Ni. Similarly the right bracket corresponds to pairs ^{128,132}Sn / ^{80,82}Ge. At least two peaks centered at the partitions marked in the figure (70/132 and 80/128 amu) are statistically significant. Actually, a parabolic (structureless) fit shown by the dot-dash line gives χ^2/f = 2.1 (chi-square per degree of freedom), while a least squares approximation by the cubic spline (dot line) shows χ^2/f = 1.04.

A peak centered at 68 amu comes out in the projection of the bump onto the M_1 axis in Fig. 9c). Further as can be inferred from Fig. 9a) the heavy fragments involved in the bump are bounded by the mass numbers in the region 128–144 associated with magic nuclei of ^{128}Sn and ^{144}Ba. This conclusion is confirmed by the projection of the bump onto the corresponding axis (Fig. 9d), where the boundaries for Sn and Ba are shown. It should be noted that the internal structure of the bump seen in Fig. 9a) is reproduced as well if the selection is made using a gate based on the drift time [30].

SUMMARY

The present work has been devoted to the observation of a new multi-body decay channel called by us "collinear cluster tri-partition" (CCT). We observe in the mass-mass distributions (2*D*) a bump linked with large missing masses in the FF mass-mass distribution for cases, where one of the fragments passes through a scattering medium providing an angular divergence between the two CCT partners flying towards the same spectrometer arm. The second principal feature of the spectrometer to be stressed is the presence of the blocking structure (grid or mesh) at the entrance to the BIC. Only due

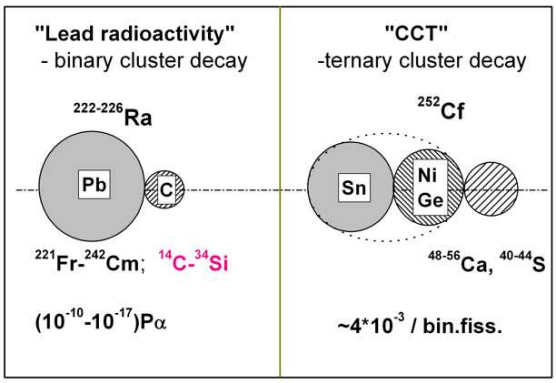

FIGURE 10. Cluster scheme for the comparison of the lead radioactivity with collinear cluster tri-partition.

to the sequential action of these two technical details, namely scattering and blocking allows the detection of a CCT event, in the frame of the missing mass method. Earlier studies of spontaneous fission of ^{252}Cf in the series of our experiments performed at different time-of-flight spectrometers [31] gave the same observation when both masses of the coincident fragments were identified in the frame of the velocity-energy (V–E) method. Bearing in mind, that potentially the scattering of fragments at the entrance to the E-detector could imitate these effects, we have used another approach with different experimental observables, being methodically independent from FF masses were needed. Such approach was realized in the other experiment Ex2 discussed in the present paper.

We have shown in Ex2 (Fig. 9), that the selection of the fission events using V–dE velocity-specific energy losses, confirmed not only the presence of the bump in the FF mass-mass distributions from the ^{235}U(n_{th}, f) reaction, but also confirmed its internal structure. In particular an effective cleaning of the bump region from the background in this case, allowed us to observe directly the tilted ridges (and, respectively, the valleys in between). These again were found to correspond to total masses of pairs of magic clusters namely (Ni/Sn) or (Ge/Sn). The ridges under discussion are actually linked with pairs of magic clusters, they are the same for the two fissioning systems, namely in ^{252}Cf and in ^{236}U*. These systems differ by 16 mass units, the position of the ridges stayed unchanged. It is believed that the ternary decay modes stand behind the tilted ridges and make clear physical sense formulated below in the "conclusions". In addition to the dE variable being absolutely independent from experimental mass values an estimation of the nuclear charge (Z) via the drift time in the ionization chambers is linked as well with the experimental fragment mass [20]. Thus the correct position of the bump in the nuclear charge of the fragments (projection on the Z axis in Fig. 8), gives clear arguments for the correctness of the origin of the bump.

CONCLUSIONS

Experimental results suggesting the existence of a new decay mode, the collinear cluster tri-partition (CCT) decay channel, have been presented. This decay mode manifests itself due to a particular bump corresponding to a specific missing mass in the FF mass-mass distributions. One of the decay modes which contribute to the bump can be treated as a new type of cluster decay as compared to the well known heavy ion or lead radioactivity. Key features of both are summed up in Fig. 10. The relatively high CCT yield can be understood if one assumes collective motion through hyper-deformed pre-scission shapes of the mother systems, which is supported by the fact that the linear arrangement realizes the lowest Coulomb potential energies of three clusters. We also emphasize, that the Q values for ternary fission are by 25–30 MeV more positive, again due to the formation of magic fragments, as in binary fission. The ternary fission process must be considered to proceed sequentially, with two neck ruptures in a short time sequence characteristic for binary fissions.

POSTSCRIPTUM

Discovering of the new type of multi-body decays of nuclei called CCT discussed here has rather long term history. First observation of the "strange" correlated events below the loci of conventional binary fission at the FOBOS setup was only first indication of the effect. Series of experiments at different time-of-flight spectrometers was needed to receive evidence that the effect is statistically reliable and well reproduced [31]. Strong arguments in favor of its physical nature presented above were obtained by attracting new experimental variables sensitive to the nuclear charge. Another experimental variable methodically independent from the fragments masses is a multiplicity of neutrons emitted in fission event. Most recent results in analysis of the neutron gated data are presented briefly below.

The experiment was performed at the FLNR of the JINR using COMETA (Correlation Mosaic E–T Array) setup [32, 33] (Fig. 11). It is double arm time-of-flight spectrometer which includes micro-channel plate (MCP) based "start" detector with the ^{252}Cf source inside, two mosaics of eight PIN diodes each and a "neutron belt" comprises 30 ^{3}He filled neutron counters. The geometry of the belt provides preferential detection of the neutrons emitted isotropically.

Fission fragments mass-mass distribution drown for the events where three neutrons (n = 3) were detected is shown in Fig. 12. The rectangle bounded by the magic nuclei attracts attention in the upper part of the figure. The tilted line corresponding to the fixed total mass of two detected fragments $M_s = M_1 + M_2 = 208$ amu (marked by the dash line) was also observed earlier.

Rectangular structure similar to this shown in Fig. 12b) was already discussed above (Fig. 9a). The evident difference between Figs. 9a) and 12b) consists in the masses of the light magic clusters namely ^{98}Sr and ^{108}Mo forming two opposite sides of the rectangle. Thus, we obtain independent confirmation of existence of the bump-like structure discussed earlier. We conclude as well that different pairs of magic clusters can be decisive for formation of the bump-like structures in the FF mass-mass distributions.

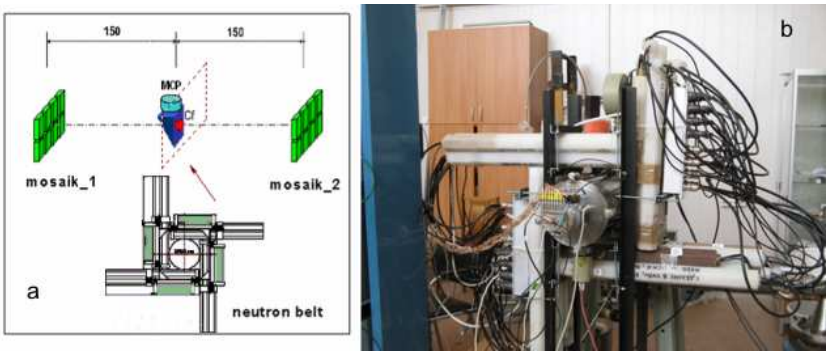

FIGURE 11. Scheme of the COMETA setup a), overall view of the spectrometer b).

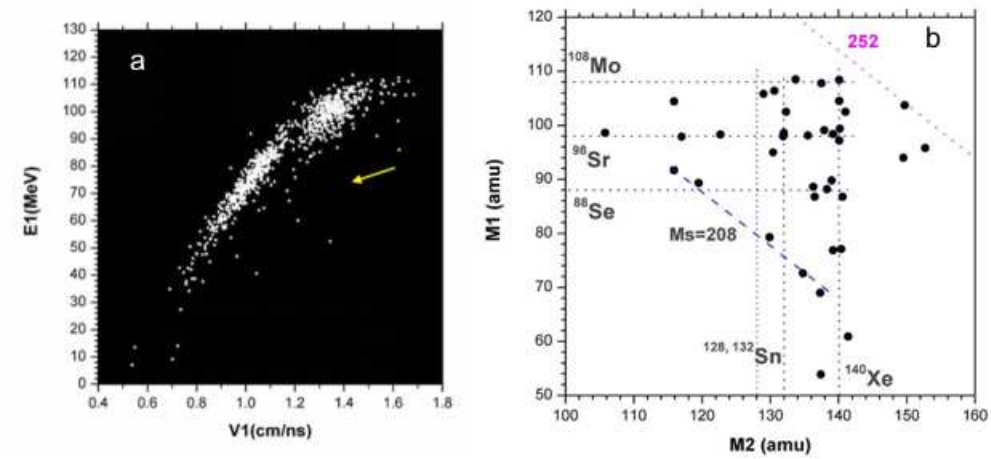

FIGURE 12. Velocity-energy distribution of the FF from ^{252}Cf (sf) under condition that three neutrons were detected in coincidence a). Mass-mass plot for the events beyond the loci of conventional binary fission in previous distribution b). Results were obtained at the COMETA setup.

It should be stressed that the COMETA setup was designed as an instrument for direct detection of all the partners of multi-body decays. Corresponding results obtained are the gratifying stuff for forthcoming presentations.

ACKNOWLEDGMENTS

This work is supported in part by the grant of the Department of Science and Technology of South Africa and by the grant of the Federal Ministry of Education and Research (BMBF) of Germany.

REFERENCES

1. O. Hahn and F. Strassmann, *Naturwissenschaften* **27**, 89–95 (1939).
2. K. A. Petrzhak and G. N. Flerov, *J. Phys.*, USSR **3**, 275–280 (1940).

3. L. Meitner and O. Frisch, *Nature* **143**, 239–240 (1939).
4. C. F. von Weizsäcker, *Z. Physik* **96**, 431–458 (1935).
5. W. J. Swiatecki, *Proceedings of the Second UN Conference on the Peaceful Uses of Atomic Energy, Geneva, 1958* United Nations, Geneva, 1958, Vol. **15**, pp. 651–659.
6. V. M. Strutinsky et al., *Nucl. Phys.* **46**, 639–659 (1963).
7. H. Diehl, W. Greiner, *Phys. Lett. B* **45**, 35–37 (1973).
8. H. Diehl, W. Greiner, *Nucl. Phys. A* **229**, 29–46 (1974).
9. D. N. Poenaru et al., *Phys. Rev. C* **59**, 3457–3460 (1999).
10. M. L. Muga, *Phys. Rev. Lett.* **11**, 129–131 (1963).
11. P. Schall et al., *Phys. Lett. B* **191**, 339–342 (1987).
12. F. Gönnenwein, *Nucl. Phys. A* **734**, 213–216 (2004).
13. S. A. Karamian et al., *Jadernaya Fizika* **5**, 959–965 (1963).
14. P. Glässel et al., *Z. Phys. A* **310**, 189–216 (1983).
15. Yu. V. Pyatkov et al., *Proceedings of the International Conference of Nuclear Physics "Nuclear Shells – 50 Years", Dubna, 1999*, edited by Yu.Ts. Oganessian et al., World Scientific, 2000, pp. 301–307.
16. Yu. V. Pyatkov et al., *Proceeding of the International Symposium on Exotic Nuclei EXON-2001, Baikal Lake, 2001*, edited by Yu. E. Penionzhkevich et al., World Scientific, 2002, pp. 181–185.
17. H.-G. Ortlepp et al., *Nucl. Instrum. Methods A* **403**, 65–97 (1998).
18. D. V. Kamanin et al., JINR Preprint Ð15-2007-182, Dubna, 2007.
19. A. Oed et al., *Nucl. Instrum. Methods* **205**, 451–453 (1983).
20. A. N. Tyukavkin et al., *Instrum. and Exp. Tech.* **52**, 508–518 (2009).
21. Yu. V. Pyatkov et al., JINR Preprint E15-2004-65, Dubna, 2004.
22. V. F. Apalin et al., *Nucl. Phys.* **71**, 553–560 (1965).
23. L. Meyer, *Physica Status Solidi (b)* **44**, 253–268 (1971).
24. A. V. Kravtsov and G. E. Solyakin, *Phys. Rev. C* **60**, 017601 (1999).
25. M. A. Mariscotti, *Nucl. Instr. and Methods* **50**, 309–320 (1967).
26. Yu. V. Pyatkov et al., *Nucl. Instr. and Methods A* **488**, 381–399 (2002).
27. B. D. Wilkins et al., *Phys. Rev. C* **14**, 1832–1863 (1976).
28. D. Rochman et al., *Nucl. Phys. A* **735**, 3–20 (2004).
29. Yu. V. Pyatkov et al., *Physics of Atomic Nuclei* **14**, 1309–1316 (2010).
30. D. V. Kamanin et al., *Int. Journal of Modern Physics E* **17**, 2250–2254 (2008).
31. Yu. V. Pyatkov et al., *Romanian Reports in Physics* **59**, 569–581 (2007).
32. Yu. V. Pyatkov et al., *Eur. Phys. J. A* **45**, 29–37 (2010).
33. D. V. Kamanin et al., *Proc. 18th International Seminar on Interaction of Neutrons with Nuclei (ISINN-18)*, 2010 in press.